Please cite the Published Version

Additional Information: This is an open access article which originally appeared in IEEE Access

RESEARCH ARTICLE

Impact of Hardware Impairment on the Uplink SIMO Cooperative NOMA With Selection Relay Under Imperfect CSI

SAFIA BEDDIAF [1], **ABDELLATIF KHELIL** [1], **FAICAL KHENNOUFA** [1],
FERDI KARA [2], **(Senior Member, IEEE), KHALED RABIE** [3,4], **(Senior Member, IEEE),**
XINGWANG LI [5], **(Senior Member, IEEE), HAKAN KAYA** [6], **AHMET EMIR** [6],
AND HALIM YANIKOMEROGLU [7], **(Fellow, IEEE)**

[1]LGEERE Laboratory, Department of Electrical Engineering, Echahid Hamma Lakhdar University, El-Oued 39000, Algeria
[2]Department of Computer Engineering, Zonguldak Bülent Ecevit University, 67100 Zonguldak, Turkey
[3]Department of Engineering, Manchester Metropolitan University, M1 5GD Manchester, U.K.
[4]Department of Electrical and Electronic Engineering Technology, University of Johannesburg, Johannesburg 2006, South Africa
[5]School of Physics and Electronic Information Engineering, Henan Polytechnic University, Jiaozuo 454000, China
[6]Department of Electrical and Electronics Engineering, Zonguldak Bülent Ecevit University, 67100 Zonguldak, Turkey
[7]Department of Systems and Computer Engineering, Carleton University, Ottawa, K1S 5B6 ON, Canada

Corresponding author: Safia Beddiaf (beddiaf-safia@univ-eloued.dz)

ABSTRACT Non-orthogonal multiple access (NOMA) has emerged as a promising solution for enabling massive connectivity in future wireless networks. A great deal of research has extensively considered the implementation of the NOMA with other technologies such as multi-antenna and cooperative communications. Most of the previous studies focused on investigating the downlink NOMA networks, while the uplink papers received relatively less attention. Besides, the majority of the current studies on uplink NOMA schemes have neglected practical limitations. Motivated by this, we investigate the uplink single-input multiple-output cooperative NOMA (SIMO-CNOMA) performance in the presence of hardware impairment (HWI), imperfect channel state information (ipCSI), and imperfect successive interference cancellation (ipSIC). We expand the scope of the proposed system to encompass multiple relay schemes, within which the selection relay technique is executed. We derive the outage probability (OP) and the system throughput of the considered system over the Rayleigh fading channels. In this respect, we provide performance analysis for different combinations of relays and antennas. The OP and system throughput analytical expressions are validated through computer simulations. In addition, the effects of HWI, ipCSI, and ipSIC on the performance of the uplink SIMO-CNOMA are discussed. The results show that the system's performance can be improved with an increase in the relays and antenna numbers. Also, there is an error floor at the high signal-to-noise ratio (SNR) in ideal conditions (i.e., in the absence of HWI, ipCSI, and ipSIC), and the error floor is increased in non-ideal conditions (i.e., in the presence of HWI, ipCSI, and ipSIC). The arbitrary number of users in the presence of non-ideal conditions increases the error and reduces the system's performance. Finally, although the performance gains obtained through the use of multiple antennas and relays, the adverse effects of HWI, ipCSI, and ipSIC on system performance cannot be avoided.

INDEX TERMS CNOMA, HWI, ipCSI, OP, SIMO, throughput.

I. INTRODUCTION

Meeting the demands of the 6th-generation (6G) and beyond wireless communication networks, which support a vast

The associate editor coordinating the review of this manuscript and approving it for publication was Stefan Schwarz.

number of connected devices with low communication latencies and improved data rates, poses a significant challenge. To address this, researchers are exploring new communication technologies and system designs. Among these technologies, non-orthogonal multiple access (NOMA) has captured the attention of the research community as

a promising solution to meet the requirements of 6G networks [1], [2]. The NOMA is based on the concept of utilizing the power domain for multiple access, which enables multiple users to be multiplexed at the same time, frequency, or code resources but at different power levels. This technique employs successive interference cancellation (SIC) to separate overlapping messages at the receiver, resulting in significant improvements in both spectrum efficiency and user fairness compared to the conventional orthogonal multiple access (OMA) [3], [4], [5]. The evaluation of performance in uplink NOMA systems is extensively discussed in [6], [7], [8], and [9], where metrics such as outage probability (OP) and ergodic capacity (EC) are commonly utilized, taking into account both perfect and imperfect channel state information (CSI).

On the other hand, cooperative communication is a successful strategy for addressing issues related to multi-path propagation, extending coverage, and improving the reliability of communication systems [10]. A combination of cooperative communication and NOMA has resulted in the development of cooperative NOMA (CNOMA) systems, which have garnered significant attention in recent papers. The OP and throughput performance of the downlink CNOMA over the Nakagami-m fading channels are evaluated in [11]. The authors in [12] evaluate the OP performance of CNOMA over the Rayleigh fading. The authors in [13] examine the effectiveness of hybrid downlink-uplink NOMA cooperative relay networks by analyzing the OP, diversity order, and throughput. In [14], underlay cognitive hybrid satellite-terrestrial for CNOMA has been analyzed for OP over Rician fading and Nakagami-m fading. Furthermore, multi-relay in NOMA systems can improve wireless network coverage, capacity, reliability, and interference reduction. These systems also enhance network resilience through redundancy and diversity. The effect of the relay selection on the performance of CNOMA is investigated in [15]. The authors of [16] present the performance of the NOMA system with the aid of multiple relays where two-stage relay selection with decode-and-forward (DF) and amplify-and-forward (AF) relaying protocols. The performance of the multiple relays assisted NOMA over the Nakagami-m fading channels is investigated in [17]. In addition, advanced approaches related to NOMA are being considered through the adoption of emerging transmission techniques, such as full-duplex communications and multi-antenna systems. The authors in [18] explore the use of NOMA with a multiple-antenna AF relaying network as a means of enhancing system performance. The performance of a two-user with simultaneous wireless information and power transfer (SWIPT) of the cooperative multiple-input single-output (MISO) NOMA system is examined in [19]. In [20], the authors study the performance of the uplink single-input multiple-output (SIMO) NOMA with joint maximum likelihood detector in terms of bit error rate.

The aforementioned studies assume ideal hardware, perfect CSI, and SIC. In realistic communication systems, the hardware transceivers suffer from several imperfections due to in-phase/quadrature (I/Q) imbalance in modulators, phase noise in local oscillators, and non-linearity power amplifiers [21], [22], [23]. The effect of the hardware impairment (HWI) on the NOMA-based relay systems over the Nakagami-m channels in terms of OP and ergodic sum rate performance is evaluated in [24] and [25]. The BER and OP performance of the CNOMA under practical assumptions where the imperfect SIC (ipSIC), imperfect channel state information (ipCSI), and hardware impairments (HWI) are investigated in [26]. In [27] and [28], downlink NOMA with cognitive radio-assisted satellite-terrestrial relay networks under joint effects of channel estimation errors and HWI has been investigated in terms of secrecy OP. In [29], the OP and intercept probability of cognitive ambient backscatter downlink NOMA internet-of-vehicle enabled maritime transportation systems communication with HWI has been examined. The ambient backscatter-downlink NOMA communication with both IQI and residual HWI has been analyzed in terms of OP and ergodic rate [30]. The authors of [22] and [31] evaluate the performance of OP and system throughput of downlink and uplink CNOMA with IpCSI and IQI.

As previously mentioned, considerable attention has been given to the downlink CNOMA system with multiple relays or/and antennas in previous literature, as in [10], [11], [12], [13], [14], [15], [16], [17], [18], and [19]. However, the uplink NOMA and CNOMA system has not garnered an equivalent level of focus. The evaluation of the uplink NOMA with and without ipCSI has been analyzed in [6], [7], [8], and [9]. Moreover, multi-antenna technology plays a crucial role in enhancing the performance of NOMA and CNOMA schemes. These schemes have been predominantly investigated for downlink improvements [19], [20], while their potential in the uplink remains absent. Also, most papers consider the effect of HWI for downlink NOMA and CNOMA schemes [27], [28], [29], [30], while it is missing in the uplink NOMA and CNOMA schemes. To the best of the authors' knowledge, the investigation of uplink SIMO-CNOMA, both with and without multiple relays has not been investigated. Besides, the practical constraints have been neglected in all previous studies of the uplink of NOMA and CNOMA. Therefore, it is important to consider the practical constraints in the uplink CNOMA for realistic evaluations. Motivated by this, the performance of the uplink SIMO-CNOMA with the aid of multiple relays and an arbitrary number of users is studied in this paper in the presence of HWI, ipCSI, and ipSIC. We analyze the OP and system throughput of our considered system.

Accordingly, the main contributions of this work can be summarized as follows:

- We examine a practical multi-user uplink NOMA scheme affected by HWI, ipCSI, and ipSIC. Our analysis includes the multi-relay scenario with the selection relay (SR) technique and explores the use of SIMO to enhance performance. The transmitter has a single antenna,

while the receiver uses multiple antennas during the cooperative scheme's two transmission phases.

- We derive the OP and system throughput of our proposed system with multiple relays and SIMO. We take into account practical constraints such as HWI, ipCSI, and ipSIC. The analytical expressions are validated by computer simulations. An asymptotic analysis of the system's performance is examined in high SNR regions. The objective of this analysis is to uncover valuable insights regarding the effects of HWI, ipCSI, and ipSIC parameters on the system's performance. The results reveal an impact of HWI, ipCSI, and ipSIC parameters on the system's performance in high SNR regions.
- The impact of the system parameters, such as HWI, ipCSI, relay number, and the number of antennas on the OP and system throughput performance of the considered schemes are extensively investigated. Numerical results show that the systems are limited by the effects of HWI and ipCSI which have a degradation on the system performance despite increases in the number of antennas and relays.

The rest of the paper is organized as follows. The proposed system is introduced in Section II. In Section III, we analyze the OP and system throughput expressions. The simulation results are presented in Section IV. Finally, Section V concludes the paper.

II. SYSTEM MODEL

We consider an uplink CNOMA system consisting of an access point (AP), J users, and L relays denoted as $\{U_j, j \in [1, J]\}$ and $\{R_l \in [1, R_L]\}$, respectively, as presented in Fig.1. It is assumed that the AP and relays are equipped with N_r receive antennas given by $\{m \in [1, N_r]\}$. The SR is supposed to be used in our system as in [32], where the selected relay denotes as R_l. The direct links between the users and the AP are neglected due to the obstacles, so the AP receives the users' signals with the help of relays. The complex Rayleigh channel coefficients between the users-relays and relays-AP are presented as $h_j^{\{m,R_l\}} \sim \mathcal{CN}(0, \gamma_j^{\{m,l\}} = d_{h_j^{m,R_l}}^{-\mu})$ and $g^{\{m,R_l\}} \sim \mathcal{CN}(0, \gamma^{\{m,R_l\}} = d_{g^{m,R_l}}^{-\mu})$, respectively, where $d_{h_j^{m,R_l}}^{-\mu}$ and $d_{g^{m,R_l}}^{-\mu}$ are distances between related nodes and μ is the path loss exponent. We assume that CSI between all nodes is imperfect and relay nodes work in half-duplex (HD) mode. The estimated channel coefficients are given as $\tilde{h}_j^{\{m,R_l\}} = h_j^{\{m,R_l\}} - e$ and $\tilde{g}^{\{m,R_l\}} = g^{\{m,R_l\}} - e$, where e is the channel estimation error as in [33]. and $e \sim \mathcal{CN}(0, \sigma_\epsilon^2)$.

Based on the uplink CNOMA scheme, in the first phase, the users transmit their signals simultaneously to the selected relay R_l. Hence, the received signal at relay l in the presence of HWI and ipCSI can be expressed as

$$y_I^{\{m,R_l\}} = \sum_{j=1} (\tilde{h}_j^{\{m,R_l\}} + e)(\sqrt{\alpha_j P} x_j + \eta_I^{\{m,R_l\}}) + n, \quad (1)$$
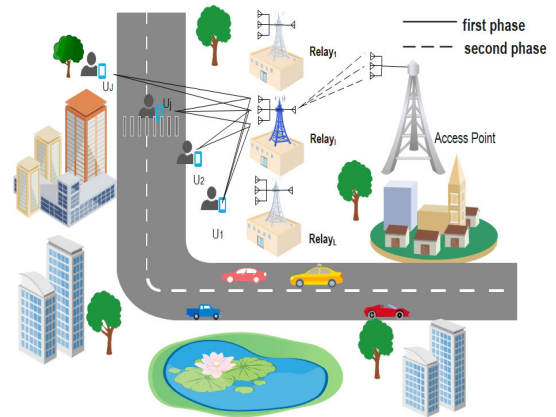

FIGURE 1. System model of uplink SIMO-CNOMA with SR.

where P is the total transmit power, α_j is power allocation (PA) coefficients in which $\alpha_j < \ldots < \alpha_3 < \alpha_2 < \alpha_1$ and $\sum_j \alpha_j = 1$, n is the additive white Gaussian noise (AWGN) $n \sim \mathcal{CN}(0, \sigma_n^2)$, x_j is the users signal with $E[|x_j|^2] = 1$, where $E[.]$ is the expectation operator.

Since R_l node has N_r antennas at the receiver, we suppose that the selection combining (SC) technique[1] is used to select the best-received signal. Thus, it is assumed the SC is implemented based on the received signal-to-interference plus noise ratios (SINR) for each signal i.e., the SIC for each antenna is performed then the SC is used to select a better received SINR. In general, the R_l node decodes the received signals using the SIC process, where the signal with a higher power (i.e., the signal of U_1) is decoded first then the signal with lower power (i.e., the signal of U_2), and so on until the last signal (i.e., the signal of U_j). The SIC is supposed to be imperfect in this paper. The received SINRs for the signal transmitted by the U_j to the R_l in the first phase can be defined as in (2), as shown at the bottom of the next page. In which $\psi_I = \sum_{j=1} k_j^{\{m,R_l\}^2} \sigma_e^2 P + \sigma_e^2 P + \sigma_n^2$, ς represents the residual SIC factor.

R_l re-combines the decoded signals of the first phase in new superimposed coding signals with different power allocations according to the channel gain as in the first phase (we assume the distribution of power in the second phase will be the same as the first phase, i.e., $\alpha_j < \ldots < \alpha_3 < \alpha_2 < \alpha_1$, where $\sum_j \alpha_j = 1$) and forward it to AP in the second phase. The received signal in the presence of HWI and ipCSI at the

---

[1]As it is known in the diversity combining techniques the maximal ratio combining (MRC) is better than SC. In the uplink CNOMA, the received signal consists of different signals coming from various sources and channels. In this case, the implementation of SC at the receiver requires less computational complexity compared to MRC to evaluate the system's performance. In the SC, the receiver chooses the signal with the highest signal-to-noise ratio (SNR) and discards the others, while in MRC, all signals are combined. Both of them are part of the diversity combining technique, which is utilized to increase the reliability of wireless communication systems. Thus, to evaluate the system performance of this paper and for less complexity, we use the SC techniques.

AP can be given as

$$y_{II}^{\{m,R_l\}} = (\tilde{g}^{\{m,R_l\}} + e)\left(\sum_{j=1}\sqrt{\alpha_j P}x_j + \eta_{II}^{\{m,R_l\}}\right) + n, \quad (3)$$

where $\eta_I^{\{m,R_l\}}$ and $\eta_{II}^{\{m,R_l\}}$ are the distortion term of the HWI at the first and the second phase which are defined respectively as in [26] with $\eta_I^{\{m,R_l\}} \sim \mathcal{CN}(0, \; k_I^{\{m,R_l\}^2}P)$ and $\eta_{II}^{\{m,R_l\}} \sim \mathcal{CN}(0, \; k_{II}^{\{m,R_l\}^2}P)$.

AP decodes the signals using the SIC process, where a higher strength signal is decoded first then a lower strength signal, and so on until the last signal (i.e., the U_1 is decoded first then U_2 and so on until U_j). In SR schemes, only one relay will be allowed to forward the signal. If relay l is selected, it will transmit the signal to the AP in the second phase. The relay whose path has the maximum SINR is selected. Since the receiver at AP has multiple antennas, it is assumed that the SC is used to select the best-received signal based on the highest SINR. Hence, the SINR at AP in the second phase can be given in (4), as shown at the bottom of the next page. In which $\psi_{II} = K^{\{m,R_l\}^2}\sigma_e^2 P + \sigma_e^2 P + \sigma_n^2$.

At the receiver of R_l and AP, the SC technique is used to select the best-received signal according to the highest received SINR. It is supposed also the SR technology is adopted, so only one path U$_j$-R_l and R_l-AP will be allowed to select, i.e., only one relay will be allowed to forward the signal to the AP. Hence, the SINR of the optimal SR for U$_j$ based on max-min relay selection criteria as in [34] can be written as

$$\Gamma_l^{SR} = \max_{R_l=R_1,\dots,R_L}\{\min\{\Gamma_{j,I}^{\{m,R_l\}}\}, \{\Gamma_{j,II}^{\{m,R_l\}}\}\}, \quad (5)$$

with

$$\Gamma_{j,I}^{\{m,R_l\}} = \max_{m=1,\dots,N_r}(\gamma_{j,I}^{\{m,R_l\}}), \quad (6)$$

$$\Gamma_{j,II}^{\{m,R_l\}} = \max_{m=1,\dots,N_r}(\gamma_{j,II}^{\{m,R_l\}}). \quad (7)$$

III. PERFORMANCE ANALYSIS

In this section, we derive the OP and system throughput expressions of the considered system under HWI, ipCSI, and ipSIC over the Rayleigh fading channel. Thus, OP and system throughput of the considered system are derived in the below subsections, respectively.

A. OUTAGE PROBABILITY

In this subsection, we derive the OP expressions of the uplink SIMO-CNOMA assisted multiple relays with an arbitrary number of users in the presence of HWI, ipCSI, and ipSIC. To

detect multiple signals in a specific order, R_l uses SIC. The SIC starts with the signal that has the highest power and ends with the signal that has the lowest power. In the first step, R_l uses maximum likelihood detection (MLD) to detect the U_1 signal. Then, the SIC is performed to detect the subsequent signals. Once the U_1 signal is detected, it is removed from the total received signal, and the same process is repeated to detect the next signal. This process is repeated for all the signals until the U_j signal is detected.

Thereafter, the R_l re-encodes the detected signals in phase one and combines them in a new superimposed coding signal, and forwards it to AP. In this latter, the detection will be according to the power allocation of each signal, in which the signal of the highest power (signal of U_1) is detected first. Then, using the SIC detects the signals that have lower powers. Assuming that the receivers are equipped with multiple antennas while the transmitter has a single antenna, in the two phases as presented in Fig. 1. It is assumed that the SC technique is used at R_l and AP to select the best-received signals according to their SINRs. Also, SR technology is used to choose the best signal transmission path according to the SINRs of each path as described in (5). The OP of each user is calculated in the subsubsections below.

1) CASE OF TWO USERS
- Outage probability of U_1: The OP of the U_1 in the phase one and two are defined as the probability of the received SINR of the U_1 is less than the threshold $\gamma_{th,1}$, where $\gamma_{th,1} = 2^{2r_1} - 1$, r_1 is the target rate of x_1. The end-2-end (e2e) OP of U_1 signal, when SR and SC are implemented under HWI and ipCSI is expressed as

$$P_1(out) = \prod_1^{R_L}\Bigg[1 - \Bigg(1 - \prod_{m=1}^{N_r}Pr\left(\gamma_{1,I}^{m,R_l} < \gamma_{th,1}\right)\Bigg) \\ \times \Bigg(1 - \prod_{m=1}^{N_r}Pr\left(\gamma_{1,II}^{\{m,R_l\}} < \gamma_{th,1}\right)\Bigg)\Bigg]. \quad (8)$$

Each term of (8) can be computed as given in (9) and (10), as shown at the bottom of the next page, respectively, shown at the top of the next page. In which $z_1 = \left(\sigma_e^2 PK_{2,I}^{\{m,R_l\}^2} + \sigma_e^2 P + \sigma_n^2\right)$, $a1 = P\left(\alpha_1 - \gamma_{th,1}K_{1,I}^{\{m,R_l\}^2}\right)$ and $b1 = P\left(\alpha_2 + K_{2,I}^{\{m,R_l\}^2}\right)$. Thus, by substituting (9) and (10) into (8), we can obtain the OP of the U_1 as given in (11), as shown at the bottom of the next page.
- Outage probability of U_2: The outage of the U_2 signal at R_l and AP occurs if they cannot successfully decode the U_1 and U_2 signals. Thus, the e2e OP of the U_2 signal under HWI, ipCSI, and ipSIC can be written

$$\gamma_{j,I}^{\{m,R_l\}} = \frac{\alpha_j P|\tilde{h}_j^{\{m,R_l\}}|^2}{\sum_{j+1}\alpha_{j+1}P|\tilde{h}_{j+1}^{\{m,R_l\}}|^2 + \sum_{i=1}^{j-1}\varsigma\alpha_i P|\tilde{h}_i^{\{m,R_l\}}|^2 + \sum_{j=1}|\tilde{h}_j^{\{m,R_l\}}|^2 k_j^{\{m,R_l\}^2}P + \psi_I}, \quad (2)$$

as in (12), as shown at the bottom of the next page. Where $\gamma_{th,2} = 2^{2r_2} - 1$, r_2 is the target rate of x_2. Hence, we can re-write (12) as

$$P_2(out) = \prod_1^{R_L} \left[1 - P_{2,I}(out)P_{2,II}(out) \right], \qquad (13)$$

where $P_{2,I}$ and $P_{2,II}$ are the OP of U_2 in the first phases and the second phase, respectively,

$$P_{2,I}(out) = \left[1 - \left(1 - \prod_{m=1}^{Nr} Pr\left(\gamma_{1,I}{}^{\{m,R_l\}} < \gamma_{th,1} \right) \right) \right.$$
$$\left. \times \left(1 - \prod_{m=1}^{Nr} Pr\left(\gamma_{2,I}{}^{\{m,R_l\}} < \gamma_{th,2} \right) \right) \right], \qquad (14)$$

and

$$P_{2,II}(out) = \left[1 - \left(1 - \prod_{m=1}^{Nr} Pr\left(\gamma_{1,II}{}^{\{m,R_l\}} < \gamma_{th,1} \right) \right) \right.$$
$$\left. \times \left(1 - \prod_{m=1}^{Nr} Pr\left(\gamma_{2,II}{}^{\{m,R_l\}} < \gamma_{th,2} \right) \right) \right]. \qquad (15)$$

Hence, each term of (14) can be computed as in (16) and (17), as shown at the bottom of the next page, as where $z_2 = \left(\sigma_e^2 P K_{1,I}^{\{m,R_l\}^2} + \sigma_e^2 P + \sigma_n^2 \right)$, $a2 = P\left(\alpha_2 - \gamma_{th,1} K_{2,I}^{\{m,R_l\}^2} \right)$ and $b2 = P\left(\varsigma\alpha_1 + K_{1,I}^{\{m,R_l\}^2} \right)$. By substituting (16) and (17) into (14), we get the OP of U_2 in the first phase as (18), as shown at the bottom of the next page. Likewise, each term in (15) can be calculated as in (19) and (20), as shown at the bottom of the next page.

By substituting (19) and (20) into (15), we get the OP of the U_2 in the second phase as in (21), as shown at the bottom of the next page. To find the e2e OP of the U_2, we substitute (18) and (21) into (13).

2) CASE OF ARBITRARY NUMBER OF USERS
In order to obtain the OP for U_j (where $1 < j < J$), it is required to determine the probability that user U_j will successfully detect both its own signal and the signals of users who are further away in the two phases (i.e., at R_l and AP). In other words, the corresponding e2e OP of U_j underHWI,

$$\gamma_{j,II}{}^{\{m,R_l\}} = \frac{\alpha_j P |\tilde{g}^{m,R_l}|^2}{\sum\limits_{j+1} \alpha_j P |\tilde{g}^{m,R_l}|^2 + \sum\limits_{i=1}^{j-1} \varsigma\alpha_i P |\tilde{g}^{\{m,R_l\}}|^2 + |\tilde{g}^{m,R_l}|^2 K^{\{m,R_l\}^2} P + \psi_{II}}, \qquad (4)$$

$$\prod_{m=1}^{Nr} Pr\left(\gamma_{1,I}^{m,R_l} < \gamma_{th,1} \right) = \prod_{m=1}^{Nr} Pr\left(|\tilde{h}_1{}^{m,R_l}|^2 < \frac{\gamma_{th,1}\left[b1|\tilde{h}_2{}^{m,R_l}|^2 + z_1 \right]}{a1} \right)$$
$$= \prod_{m=1}^{Nr} \left(1 - \exp\left(-\frac{z_1\gamma_{th,1}}{a1\lambda_{h_1{}^{m,R_l}}} \right) \frac{a1\lambda_{h_1{}^{m,R_l}}}{b1\gamma_{th,1}\lambda_{h_2{}^{m,R_l}} + a1\lambda_{h_1{}^{m,R_l}}} \right), \qquad (9)$$

$$\prod_{m=1}^{Nr} Pr\left(\gamma_{1,II}^{\{m,R_l\}} < \gamma_{th,1} \right) = \prod_{m=1}^{Nr} Pr\left(|\tilde{g}^{\{m,R_l\}}|^2 < \frac{\gamma_{th,1}\psi_{II}}{\left(\alpha_1 P - \gamma_{th,1}\alpha_2 P - \gamma_{th,1}K_{II}^{\{m,R_l\}^2} P \right)} \right)$$
$$= \prod_{m=1}^{Nr} \left(1 - \exp\left(-\frac{\gamma_{th,1}\psi_{II}}{\lambda_{g^{\{m,R_l\}}}\left(\alpha_1 P - \gamma_{th,1}\alpha_2 P - \gamma_{th,1}K_{II}^{\{m,R_l\}^2} P \right)} \right) \right), \qquad (10)$$

$$P_1(out) = \prod_1^{R_L} \left[1 - \left(1 - \prod_{m=1}^{Nr} \left(1 - \exp\left(-\frac{z_1\gamma_{th,1}}{a1\lambda_{h_1{}^{m,R_l}}} \right) \frac{a1\lambda_{h_1{}^{m,R_l}}}{b1\gamma_{th,1}\lambda_{h_2{}^{m,R_l}} + a1\lambda_{h_1{}^{m,R_l}}} \right) \right) \right.$$
$$\left. \times \left(1 - \prod_{m=1}^{Nr} \left(1 - \exp\left(-\frac{\gamma_{th,1}\left(\sigma_e^2 P \left(K_{II}^{\{m,R_l\}^2} + 1 \right) + \sigma_n^2 \right)}{\lambda_{g^{\{m,R_l\}}}\left(\alpha_1 P - \gamma_{th,1}\alpha_2 P - \gamma_{th,1}K_{II}^{\{m,R_l\}^2} P \right)} \right) \right) \right) \right]. \qquad (11)$$

ipCSI, and ipSIC can be computed as

$$
\begin{aligned}
&P_j(out) \\
&= \prod_{1}^{R_L}\Bigg[1 - \Bigg[1 - \prod_{j=1}^{J}\Bigg(1 - \prod_{m=1}^{Nr} Pr\left(\gamma_{j,I}{}^{\{m,R_l\}} < \gamma_{th,j}\right)\Bigg)\Bigg] \\
&\quad \times \Bigg[1 - \prod_{j=1}^{J}\Bigg(1 - \prod_{m=1}^{Nr} Pr\left(\gamma_{j,II}^{\{m,R_l\}} < \gamma_{th,1}\right)\Bigg)\Bigg]\Bigg],
\end{aligned} \tag{22}
$$

where $\gamma_{th,j} = 2^{2r_j} - 1$, r_j is the target rate of x_j. Hence, (22) can be re-written as

$$
P_j(out) = \prod_{1}^{R_L}\Bigg[1 - \prod_{j=1}^{J} P_{j,I}(out)\prod_{j=1}^{J} P_{j,II}(out)\Bigg], \tag{23}
$$

where

$$
P_{j,I}(out) = 1 - \prod_{j=1}^{J}\Bigg(1 - \prod_{m=1}^{Nr} Pr\left(\gamma_{j,I}^{\{m,R_l\}} < \gamma_{th,j}\right)\Bigg), \tag{24}
$$

$$
\begin{aligned}
P_2(out) = \prod_{1}^{R_L}\Bigg[1 &- \Bigg[1 - \Bigg(1 - \prod_{m=1}^{Nr} Pr\left(\gamma_{1,I}^{\{m,R_l\}} < \gamma_{th,1}\right)\Bigg)\Bigg(1 - \prod_{m=1}^{Nr} Pr\left(\gamma_{2,I}^{\{m,R_l\}} < \gamma_{th,2}\right)\Bigg)\Bigg] \\
&\times \Bigg[1 - \Bigg(1 - \prod_{m=1}^{Nr} Pr\left(\gamma_{1,II}^{\{m,R_l\}} < \gamma_{th,1}\right)\Bigg)\Bigg(1 - \prod_{m=1}^{Nr} Pr\left(\gamma_{2,II}^{\{m,R_l\}} < \gamma_{th,2}\right)\Bigg)\Bigg]\Bigg],
\end{aligned} \tag{12}
$$

$$
Pr\left(\gamma_{1,I}{}^{\{m,R_l\}} < \gamma_{th,1}\right) = \prod_{m=1}^{Nr}\Bigg[1 - \exp\Bigg(-\frac{z_1\gamma_{th,1}}{a1\lambda_{h_1^{m,R_l}}}\Bigg)\frac{a1\lambda_{h_1^{\{m,R_l\}}}}{b1\gamma_{th,1}\lambda_{h_2^{\{m,R_l\}}} + a1\lambda_{h_1^{\{m,R_l\}}}}\Bigg], \tag{16}
$$

$$
Pr\left(\gamma_{2,I}^{\{m,R_l\}} < \gamma_{th,2}\right) = \prod_{m=1}^{Nr}\Bigg[1 - \exp\Bigg(-\frac{z_2\gamma_{th,2}}{a2\lambda_{h_2^{m,R_l}}}\Bigg)\frac{a2\lambda_{h_2^{\{m,R_l\}}}}{b2\gamma_{th,2}\lambda_{h_1^{\{m,R_l\}}} + a2\lambda_{h_2^{\{m,R_l\}}}}\Bigg], \tag{17}
$$

$$
\begin{aligned}
P_{2,I}(out) = 1 &- \Bigg(1 - \prod_{m=1}^{Nr}\Bigg[1 - \exp\Bigg(-\frac{z_1\gamma_{th,1}}{a1\lambda_{h_1^{m,R_l}}}\Bigg)\frac{a1\lambda_{h_1^{\{m,R_l\}}}}{b1\gamma_{th,1}\lambda_{h_2^{\{m,R_l\}}} + a1\lambda_{h_1^{\{m,R_l\}}}}\Bigg]\Bigg) \\
&\times \Bigg(1 - \prod_{m=1}^{Nr}\Bigg[1 - \exp\Bigg(-\frac{z_2\gamma_{th,2}}{a2\lambda_{h_2^{m,R_l}}}\Bigg)\frac{a2\lambda_{h_2^{\{m,R_l\}}}}{b2\gamma_{th,2}\lambda_{h_1^{\{m,R_l\}}} + a2\lambda_{h_2^{\{m,R_l\}}}}\Bigg]\Bigg).
\end{aligned} \tag{18}
$$

$$
Pr\left(\gamma_{1,II}^{\{m,R_l\}} < \gamma_{th,1}\right) = \prod_{m=1}^{Nr}\Bigg[1 - \exp\Bigg(-\frac{\gamma_{th,1}\psi_{II}}{\lambda_{g^{\{m,R_l\}}}}\left(\alpha_1 P - \gamma_{th,1}\alpha_2 P - \gamma_{th,1}K_{II}^{\{m,R_l\}^2} P\right)\Bigg)\Bigg], \tag{19}
$$

$$
Pr\left(\gamma_{2,II}^{\{m,R_l\}} < \gamma_{th,2}\right) = \prod_{m=1}^{Nr}\Bigg[1 - \exp\Bigg(-\frac{\gamma_{th,2}\psi_{II}}{\lambda_{g^{\{m,R_l\}}}\left(\alpha_2 P - \gamma_{th,2}\varsigma\alpha_1 P - \gamma_{th,2}K_{II}^{\{m,R_l\}^2} P\right)}\Bigg)\Bigg]. \tag{20}
$$

$$
\begin{aligned}
P_{2,II}(out) = 1 &- \Bigg(1 - \prod_{m=1}^{Nr}\Bigg[1 - \exp\Bigg(-\frac{\gamma_{th,1}\psi_{II}}{\lambda_{g^{\{m,R_l\}}}}\left(\alpha_1 P - \gamma_{th,1}\alpha_2 P - \gamma_{th,1}K_{II}^{\{m,R_l\}^2} P\right)\Bigg)\Bigg]\Bigg) \\
&\times \Bigg(1 - \prod_{m=1}^{Nr}\Bigg[1 - \exp\Bigg(-\frac{\gamma_{th,2}\psi_{II}}{\lambda_{g^{\{m,R_l\}}}\left(\alpha_2 P - \gamma_{th,2}\varsigma\alpha_1 P - \gamma_{th,2}K_{II}^{\{m,R_l\}^2} P\right)}\Bigg)\Bigg]\Bigg).
\end{aligned} \tag{21}
$$

(a) Case of one relay   (b) Case of two relays   (c) Case of three relays
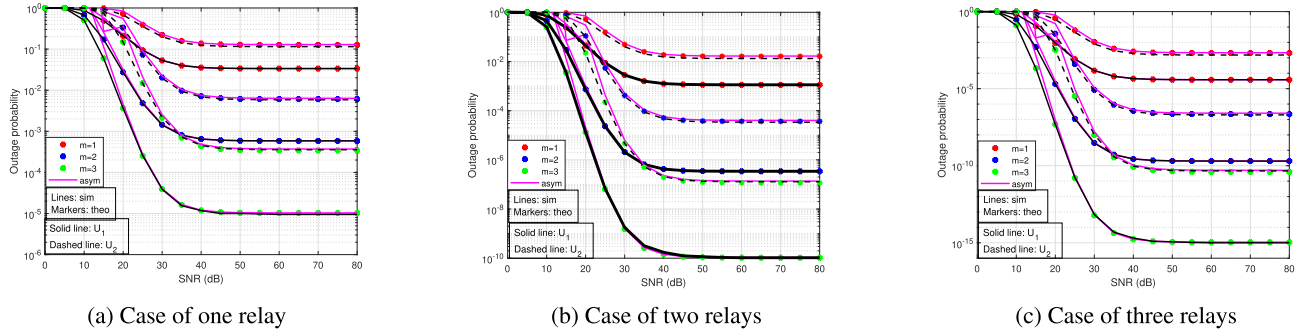
FIGURE 2. OP w.r.t. SNR for uplink SIMO-CNOMA with SR of two users.

(a) Case of one relay   (b) Case of two relays   (c) Case of three relays
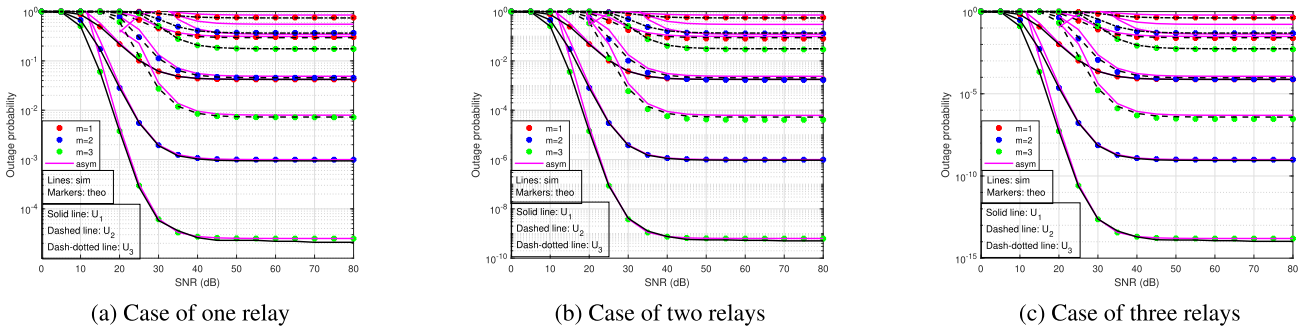
FIGURE 3. OP w.r.t. SNR for uplink SIMO-CNOMA with SR of three users.

and

$$P_{j,II}(out) = 1 - \prod_{j=1}^{J}\left(1 - \prod_{m=1}^{Nr} Pr\left(\gamma_{j,II}^{\{m,R_l\}} < \gamma_{th,j}\right)\right), \tag{25}$$

where $P_{j,I}(out)$ and $P_{j,II}(out)$ are the OP of U_j in the first and the second phases, respectively. The term of (24) can be calculated as in (26), as shown at the bottom of the next page.

    Proof: Please see Appendix A.   ∎

The term of (25) can be calculated as given in (27), as shown at the bottom of the next page. By using the probability density functions (PDF) and cumulative distribution function (CDF) of Rayleigh fading, which are defined in [10], (27) can be obtained as in (28), as shown at the bottom of the next page. Thus, to find the OP of the first and the second phase of U_j, we substitute (26) and (28) into (24) and (25), respectively. Finally, to obtain the e2e OP of U_j we substitute (24) and (25) into (23).

B. ASYMPTOTIC OUTAGE PROBABILITY
In this subsection, we investigate the behavior of the asymptotic OP in high SNR regimes which can be defined as $\exp(-x) \approx (1-x)$ as in [35], and [26] to gain insights into our considered scenarios.

1) CASE OF TWO USERS
The asymptotic OP of the U_1 is given in (29), as shown at the bottom of the next page. In order to obtain the asymptotic

OP of the U_2, we need to find the OP of the first and second phases as given in (30), as shown at the bottom of the next page, and (31), as shown at the bottom of page 9. Replacing (30) and (31) into (13), we find the asymptotic OP of the U_2.

2) CASE OF ARBITRARY NUMBER OF USERS
To obtain the asymptotic OP of U_j, we need to find the asymptotic OP of the first and second phases as given in (32) and (33), as shown at the bottom of page 9. Substituting (32) and (33) into (24) and (25) to find the asymptotic OP of the first and second phases of the U_j, respectively. Thus, the asymptotic OP of the U_j can be expressed by replacing the asymptotic OP of the first and second phases into (23).

C. SYSTEM THROUGHPUT
In this subsection, we provide the analytical expression of the system throughput which is expressed as [22]

$$\zeta = \sum_{j=1}^{J}(1 - P_j(out))r_j, \tag{34}$$

where $P_j(out)$ is the e2e OP of U_j.

IV. NUMERICAL RESULTS
In this section, the analytical OP and system throughput expressions are validated by computer simulations. Particularly, we investigate the impact of the HWI, ipCSI, and ipSIC on the uplink SIMO-CNOMA with SR and an arbitrary number of users. The simulation results in all figures match

$$
\prod_{m=1}^{Nr} Pr\left(\gamma_{j,I}^{\{m,R_l\}} < \gamma_{th,j}\right) = \prod_{m=1}^{Nr}\left(1 - \exp\left(-\frac{\gamma_{th,j}z_j}{P(\alpha_j - \gamma_{th,j}k_j^{\{m,R_l\}^2})\lambda_{h_j^{\{m,R_l\}}}}\right)\right.
$$
$$
\times \frac{P(\alpha_j - \gamma_{th,j}k_j^{\{m,R_l\}^2})\lambda_{h_j^{\{m,R_l\}}}}{P(\alpha_j - \gamma_{th,j}k_j^{\{m,R_l\}^2})\lambda_{h_j^{\{m,R_l\}}} + \gamma_{th,j}(\alpha_{j+1} + k_{j+1}^{\{m,R_l\}^2})\, P\, \lambda_{h_{j+1}^{\{m,R_l\}}}}
$$
$$
\times \frac{P(\alpha_j - \gamma_{th,j}k_j^{\{m,R_l\}^2})\lambda_{h_j^{\{m,R_l\}}}}{P(\alpha_j - \gamma_{th,j}k_j^{\{m,R_l\}^2})\lambda_{h_j^{\{m,R_l\}}} + \gamma_{th,j}(\varsigma\alpha_{(j-1)} + k_{(j-1)}^{\{m,R_l\}^2})\, P\, \lambda_{h_{j-1}^{\{m,R_l\}}}}
$$
$$
\times \frac{P(\alpha_j - \gamma_{th,j}k_j^{\{m,R_l\}^2})\lambda_{h_j^{\{m,R_l\}}}}{P(\alpha_j - \gamma_{th,j}k_j^{\{m,R_l\}^2})\lambda_{h_j^{\{m,R_l\}}} + \gamma_{th,j}(\alpha_{j+2} + k_{j+2}^{\{m,R_l\}^2})\, P\, \lambda_{h_{j+2}^{\{m,R_l\}}}}
$$
$$
\times \frac{P(\alpha_j - \gamma_{th,j}k_j^{\{m,R_l\}^2})\lambda_{h_j^{\{m,R_l\}}}}{P(\alpha_j - \gamma_{th,j}k_j^{\{m,R_l\}^2})\lambda_{h_j^{\{m,R_l\}}} + \gamma_{th,j}(\varsigma\alpha_{j-2} + k_{j-2}^{\{m,R_l\}^2})\, P\, \lambda_{h_{j-2}^{\{m,R_l\}}}}
$$
$$
\ldots \times \frac{P(\alpha_j - \gamma_{th,j}k_j^{\{m,R_l\}^2})\lambda_{h_j^{\{m,R_l\}}}}{P(\alpha_j - \gamma_{th,j}k_j^{\{m,R_l\}^2})\lambda_{h_j^{\{m,R_l\}}} + \gamma_{th,j}(\alpha_J + k_J^{\{m,R_l\}^2})\, P\, \lambda_{h_J^{\{m,R_l\}}}}
$$
$$
\times \left.\frac{P(\alpha_j - \gamma_{th,j}k_j^{\{m,R_l\}^2})\lambda_{h_j^{\{m,R_l\}}}}{P(\alpha_j - \gamma_{th,j}k_j^{\{m,R_l\}^2})\lambda_{h_j^{\{m,R_l\}}} + \gamma_{th,j}(\varsigma\alpha_{(J-1)} + k_{J-1}^{\{m,R_l\}^2})\, P\, \lambda_{h_{J-1}^{\{m,R_l\}}}}\right). \tag{26}
$$

$$
\prod_{m=1}^{Nr} Pr\left(\gamma_{j,II}^{\{m,R_l\}} < \gamma_{th,j}\right) = \prod_{m=1}^{Nr} Pr\left(|\tilde{g}^{m,R_l}|^2 < \frac{\gamma_{th,j}\psi_{II}}{P(\alpha_j - \gamma_{th,j}\sum_{j+1}\alpha_{j+1} - \gamma_{th,j}\sum_{i=1}^{j+1}\varsigma\alpha_i - \gamma_{th,j}K_{II}^{\{m,R_l\}^2})}\right). \tag{27}
$$

$$
\prod_{m=1}^{Nr} Pr\left(\gamma_{j,II}^{\{m,R_l\}} < \gamma_{th,j}\right) = \prod_{m=1}^{Nr}\left(1 - \exp\left(-\frac{\gamma_{th,j}\psi_{II}}{P(\alpha_j - \gamma_{th,j}\sum_{j+1}\alpha_{j+1} - \gamma_{th,j}\sum_{i=1}^{j+1}\varsigma\alpha_i - \gamma_{th,j}K^{\{m,R_l\}^2})\lambda_{g^{\{m,R_l\}}}}\right)\right). \tag{28}
$$

$$
P_1^{asy}(out) \approx \prod_1^{R_L}\left[1 - \left(1 - \prod_{m=1}^{Nr}\left(\left(\frac{z_1\gamma_{th,1}}{a1\lambda_{h_1^{m,R_l}}}\right)\frac{a1\lambda_{h_1^{m,R_l}}}{b1\gamma_{th,1}\lambda_{h_2^{m,R_l}} + a1\lambda_{h_1^{m,R_l}}}\right)\right)\right.
$$
$$
\times \left.\left(1 - \prod_{m=1}^{Nr}\left(\frac{\gamma_{th,1}\psi_{II}}{\lambda_{h_1^{\{m,R_l\}}}\left(\alpha_1 P - \gamma_{th,1}\alpha_2 P - \gamma_{th,1}K_{II}^{\{m,R_l\}^2}P\right)}\right)\right)\right]. \tag{29}
$$

$$
P_{2,I}^{asy}(out) \approx 1 - \left(1 - \prod_{m=1}^{Nr}\left(\left(\frac{z_1\gamma_{th,1}}{a1\lambda_{h_1^{m,R_l}}}\right)\frac{a1\lambda_{h_1^{\{m,R_l\}}}}{b1\gamma_{th,1}\lambda_{h_2^{\{m,R_l\}}} + a1\lambda_{h_1^{\{m,R_l\}}}}\right)\right)
$$
$$
\times \left(1 - \prod_{m=1}^{Nr}\left(\left(\frac{z_2\gamma_{th,2}}{a2\lambda_{h_2^{m,R_l}}}\right)\frac{a2\lambda_{h_2^{\{m,R_l\}}}}{b2\gamma_{th,2}\lambda_{h_1^{\{m,R_l\}}} + a2\lambda_{h_2^{\{m,R_l\}}}}\right)\right). \tag{30}
$$

TABLE 1. Simulations parameters.

| parameter	value
The path loss exponent	4
Distance between the 2 users and relays	$d_{h_1} = 3m \ d_{h_2} = 5m$
Distance between the 3 users and relays	$d_{h_1} = 3m \ d_{h_2} = 4m \ d_{h_3} = 5m$
Distance between the relays and AP	$d_g = 4m$
The PA in case of 2 users	$\alpha_1 = 0.75 \ \alpha_2 = 0.25$
The PA in case of 3 users	$\alpha_1 = 0.7 \ \alpha_2 = 0.2 \ \alpha_3 = 0.1$
The HWI coefficient $K_{j,I}^{m,R_l \ 2} = K_{II}^{m,R_l \ 2}$	0.05
The channel estimation error σ_e^2	0.001
The residual SIC factor ς	0.001

perfectly with the numerical results. To validate our analysis, the parameters are set as in Tab.1.

In Fig. 2, we present the OP performance of the uplink SIMO-CNOMA system with SR for two users under HWI, ipCSI, and ipSIC versus SNR with different numbers of relays and users when $l = 1, 2, 3$ and $j = 1, 2, 3$. The asymptotic OP curves given for the two users at the high SNR are limited over the theoretical curves. We observe that the OP performance of the users improves as the number of relays and antennas increases. There is an error floor at all curves of the users despite the increase in the number of relays and antennas. NOMA supports more users, so we evaluate the OP performance with more than two users. In Fig.3, we present an evaluation of the OP performance of the uplink SIMO-CNOMA system with three users under HWI, ipCSI, and

$$P_{2,II}^{asy}(out) \approx 1 - \left(1 - \prod_{m=1}^{Nr} \left(\frac{\gamma_{th,1}\psi_{II}}{\lambda_{g\{m,R_l\}}} \left(\alpha_1 P - \gamma_{th,1}\alpha_2 P - \gamma_{th,1}K_{II}^{\{m,R_l\}^2}P \right) \right) \right)$$
$$\times \left(1 - \prod_{m=1}^{Nr} \left(\frac{\gamma_{th,2}\psi_{II}}{\lambda_{g\{m,R_l\}} \left(\alpha_2 P - \gamma_{th,2}\varsigma\alpha_1 P - \gamma_{th,2}K_{II}^{\{m,R_l\}^2}P \right)} \right) \right). \quad (31)$$

$$\prod_{m=1}^{Nr} Pr\left(\gamma_{j,I}^{\{m,R_l\}} < \gamma_{th,j} \right) \approx \prod_{m=1}^{Nr} \left(\left(\frac{\gamma_{th,j}z_j}{P(\alpha_j - \gamma_{th,j}k_j^{\{m,R_l\}^2})\lambda_{h_j\{m,R_l\}}} \right) \right.$$
$$\times \frac{P(\alpha_j - \gamma_{th,j}k_j^{\{m,R_l\}^2})\lambda_{h_j\{m,R_l\}}}{P(\alpha_j - \gamma_{th,j}k_j^{\{m,R_l\}^2})\lambda_{h_j\{m,R_l\}} + \gamma_{th,j}(\alpha_{j+1} + k_{j+1}^{\{m,R_l\}^2}) P \lambda_{h_{j+1}\{m,R_l\}}}$$
$$\times \frac{P(\alpha_j - \gamma_{th,j}k_j^{\{m,R_l\}^2})\lambda_{h_j\{m,R_l\}}}{P(\alpha_j - \gamma_{th,j}k_j^{\{m,R_l\}^2})\lambda_{h_j\{m,R_l\}} + \gamma_{th,j}(\varsigma\alpha_{j-1} + k_{j-1}^{\{m,R_l\}^2}) P \lambda_{h_{j-1}\{m,R_l\}}}$$
$$\times \frac{P(\alpha_j - \gamma_{th,j}k_j^{\{m,R_l\}^2})\lambda_{h_j\{m,R_l\}}}{P(\alpha_j - \gamma_{th,j}k_j^{\{m,R_l\}^2})\lambda_{h_j\{m,R_l\}} + \gamma_{th,j}(\alpha_{j+2} + k_{j+2}^{\{m,R_l\}^2}) P \lambda_{h_{j+2}\{m,R_l\}}}$$
$$\times \frac{P(\alpha_j - \gamma_{th,j}k_j^{\{m,R_l\}^2})\lambda_{h_j\{m,R_l\}}}{P(\alpha_j - \gamma_{th,j}k_j^{\{m,R_l\}^2})\lambda_{h_j\{m,R_l\}} + \gamma_{th,j}(\varsigma\alpha_{j-2} + k_{j-2}^{\{m,R_l\}^2}) P \lambda_{h_{j-2}\{m,R_l\}}}$$
$$\cdots \times \frac{P(\alpha_j - \gamma_{th,j}k_j^{\{m,R_l\}^2})\lambda_{h_j\{m,R_l\}}}{P(\alpha_j - \gamma_{th,j}k_j^{\{m,R_l\}^2})\lambda_{h_j\{m,R_l\}} + \gamma_{th,j}(\alpha_J + k_J^{\{m,R_l\}^2}) P \lambda_{h_J\{m,R_l\}}}$$
$$\times \left. \frac{P(\alpha_j - \gamma_{th,j}k_j^{\{m,R_l\}^2})\lambda_{h_j\{m,R_l\}}}{P(\alpha_j - \gamma_{th,j}k_j^{\{m,R_l\}^2})\lambda_{h_j\{m,R_l\}} + \gamma_{th,j}(\varsigma\alpha_{(J-1)} + k_{J-1}^{\{m,R_l\}^2}) P \lambda_{h_{J-1}\{m,R_l\}}} \right). \quad (32)$$

$$\prod_{m=1}^{Nr} Pr\left(\gamma_{j,II}^{\{m,R_l\}} < \gamma_{th,j} \right) \approx 1 - \prod_{j=1}^{J} \left(1 - \prod_{m=1}^{Nr} \left(\frac{\gamma_{th,j}\psi_{II}}{P(\alpha_j - \gamma_{th,j}\sum_{j+1}\alpha_{j+1} - \gamma_{th,j}\sum_{i=1}^{j+1}\varsigma\alpha_i - \gamma_{th,j}K^{\{m,R\}^2})\lambda_{g\{m,R_l\}}} \right) \right). \quad (33)$$
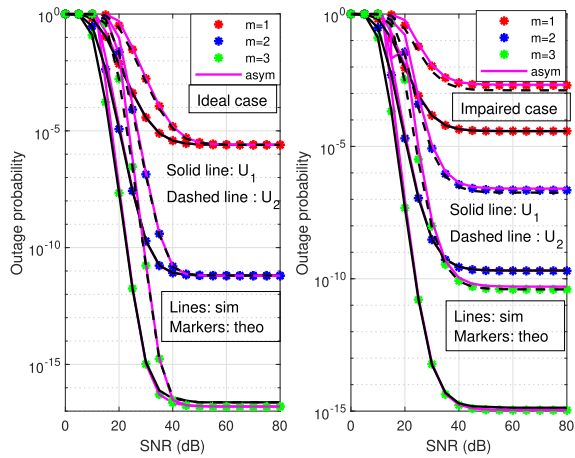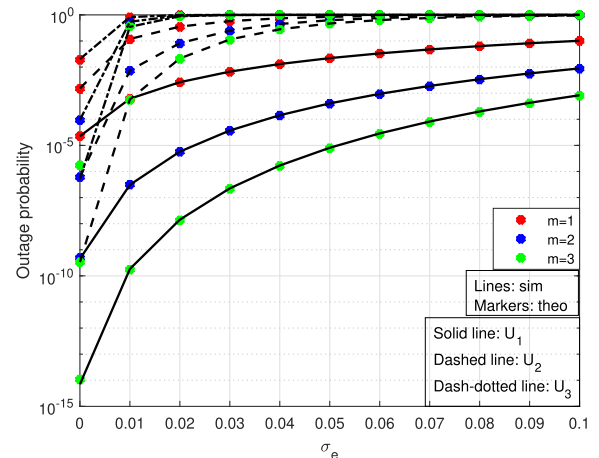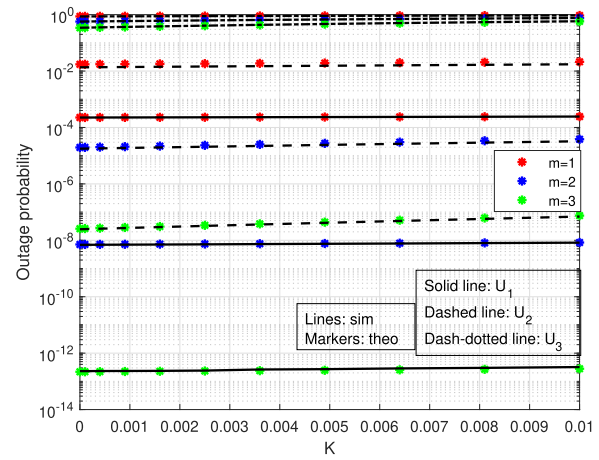
(a) Case of two users.
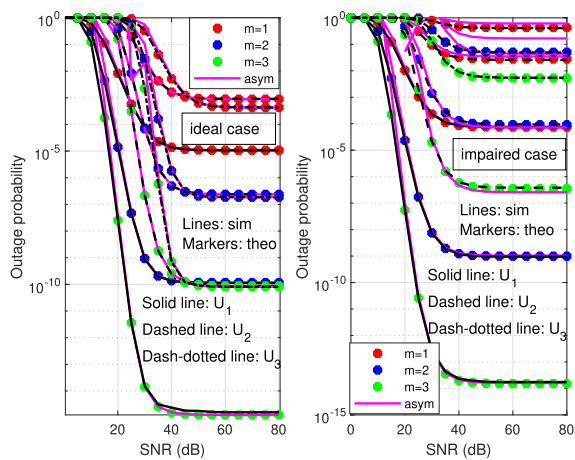
(b) Case of three users.

FIGURE 4. OP versus SNR for uplink SIMO-CNOMA comparison with the ideal case.

(a) OP w.r.t ipCSI

(b) OP w.r.t HWI

FIGURE 5. OP performance evaluation for ipCSI and HWI for uplink SIMO-CNOMA.

ipSIC versus SNR with different numbers of relays and users when $l = 1, 2, 3$ and $j = 1, 2, 3$. The asymptotic OP curves for the three users are limited within the theoretical curves, specifically in high SNR scenarios. It is observed that the users' performance improves as the antenna and relay number increase. However, there is an error floor in the high SNR regime as in Fig. 2 (case of two users), which can be attributed to two primary factors. The first factor is the interference between the users' channels. The OP in the uplink CNOMA depends on the first and second phases. As we know, in the uplink CNOMA schemes in the first phase, all users transmit their signals with different power simultaneously to the R_l node, so different signals are received at R_l node from different users with different channel quality, and this causes interference between users channel which lead to errors in the signals detecting during the SIC process, especially at high SNR. Secondly, the imperfections in the system from HWI and ipCSI also contribute to the error floor. Through the comparison between Fig. 2 and 3, we observe that the OP with two users under the HWI, ipCSI, and ipSIC is better than the

case of three users. In the case of three users, it can be easily seen that the performance of the U_3 was greatly affected than the other users, as it records a very poor performance in the presence of practical imperfections (HWI, ipCSI, and ipSIC). In these imperfections, regardless of increasing the number of relays and antennas, the performance of U_3 does not improve well. In the case of two users, the two users have good performance, and they become better when the number of relays and antennas increases in the presence of practical imperfections. The increasing number of users affects the distribution of power to the rest of the users, which affects the SIC process. The presence of practical imperfections with more users reduces the system's performance. Fig. 4 presents the OP of the uplink SIMO-CNOMA with two and three users under ideal and non-ideal conditions (HWI, ipCSI, and ipSIC) when $l = 3$ with two and three users. The performance of the users improves as the antenna number increases, and there is an error floor at the high SNR. In the non-ideal case, we observe that the presence of the HWI and ipCSI increases the error floor of the users' signals. However, the effect of HWI and ipCSI was bigger in the
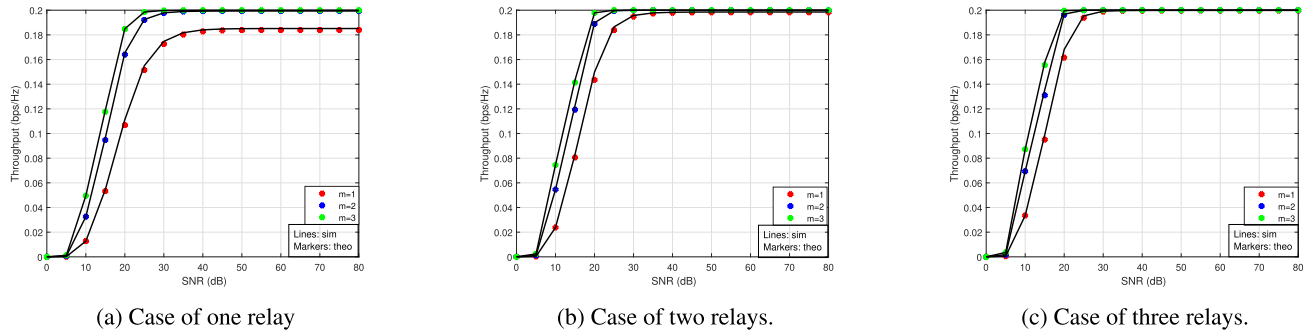
(a) Case of one relay

(b) Case of two relays.

(c) Case of three relays.

FIGURE 6. Throughput w.r.t. SNR for uplink SIMO-CNOMA with SR of two users.

(a) Case of one relay

(b) Case of two relays.
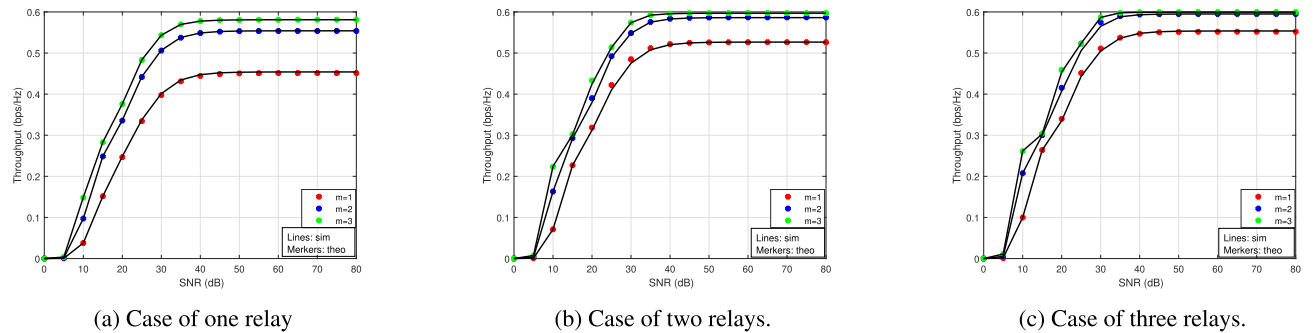
(c) Case of three relays.

FIGURE 7. Throughput w.r.t. SNR for uplink SIMO-CNOMA with SR of three users.

case of the three users than in the case of the two users, especially at the U_3. As we know, in the uplink CNOMA scheme, the OP depends on the first and second phases. Thus, the error floor comes from the first or second phases or both. Through previous analysis in the literature, when there are no interference channels as in the downlink NOMA schemes [26], there is no error floor in the ideal case. Based on that the error floor comes from the first phase in the uplink SIMO-CNOMA, where multiple users with different channels are sent their signals simultaneously to R_l node. The interference of channels occurs at the R_l node which affects the SIC and causes an error floor on the users' signals with growth SNR. In the practical imperfections (HWI, ipCSI, and ipSIC) case, it can be seen that the OP performance of the system gets worse, and the U_3 has a poor OP performance that is close to 1 despite increasing antennas number. It proves the previous discussions in Fig. 2 and 3, that the imperfections of HWI and ipCSI contribute to the error floor in the system performance, and the more number of users affects the system performance of the users.

The impact of the channel estimation error and HWI factors on OP performance with SNR = 20 dB are evaluated in Figs. 5(a) and 5(b), respectively when $l = 3$ and $j = 3$. We can observe that increasing the channel estimation error and HWI factors decreases the OP performance of all users. It can be easily seen that the HWI has less effect on the outage performance compared to the ipCSI effects with all antenna numbers. The U_3 diminishes very

quickly with an increase ipCSI factor compared to the HWI factor although the increase in antenna number. This implies that the performance of the system depends more significantly on channel estimation error than on HWI. However, the presence of HWI and ipCSI affect the SIC and the detection signals. It is clear that the large number of users in the presence of practical imperfections will affect the performance of users more. Because it reduces the power allocation of users and causes complexity in the detection. Under these circumstances, with the effects of practical imperfections, the error will be greater, so it is recommended to use fewer number users to obtain better performance. This proves the validity of previous analyzes of NOMA schemes as [36] and [37] (downlink NOMA schemes), that a large number of users reduces performance and increases error.

In Fig.6, we illustrate the system throughput of the uplink SIMO-CNOMA with different numbers of relays and antenna in the presence of HWI, ipcSI, and ipSIC w.r.t SNR when $l = 1, 2, 3$ and $j = 1, 2$. We can observe that by increasing the number of relays and antennas the system throughput improves. In another scenario, when there are more than two users, in Fig. 7, the system throughput of the uplink SIMO-CNOMA with SR in the presence of HWI, ipCSI, and ipSIC with a different number of relays and users when $l = 1, 2, 3$ and $j = 1, 2, 3$. It is observed that the throughput performance increases as the relay and antenna numbers increase. By comparing Fig. 6 and 7, it can be easily seen
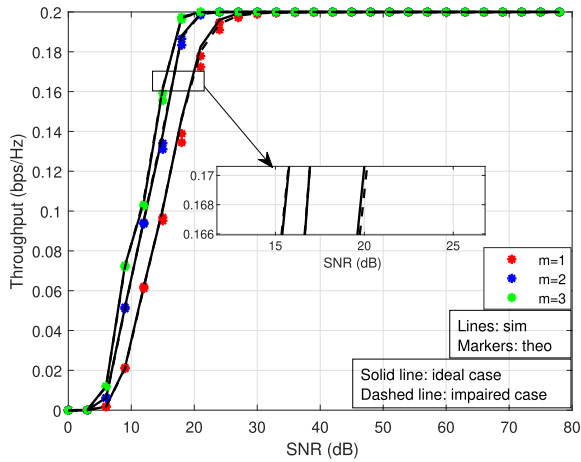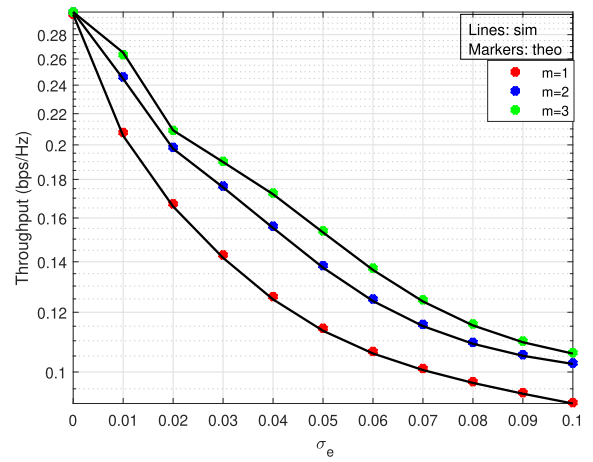
(a) Case of two users.
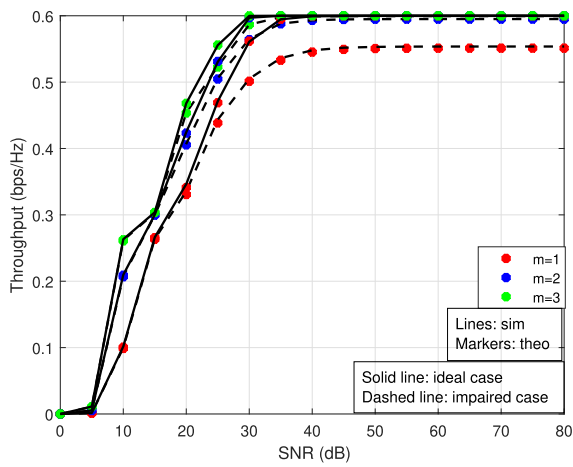
(b) Case of three users.

FIGURE 8. Throughput versus SNR for uplink SIMO-CNOMA comparison with the ideal case.

(a) Throughput w.r.t. ipCSI.

(b) Throughput w.r.t. HWI.

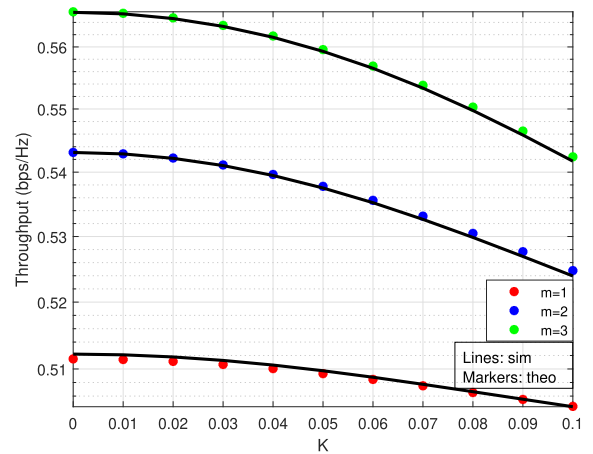**FIGURE 9.** Throughput performance evaluation for ipCSI and HWI.

that increasing the number of users increases the system throughput performance.

To examine the impact of imperfections (HWI and ipCSI) on the system throughput performance, Fig. 8 presents the uplink SIMO-CNOMA when $l = 1, 2, 3$ in the case of two and three users. We can observe that the system throughput of the ideal HWI and ipCSI ($K = 0$ and $\sigma_e^2 = 0$) achieves a higher performance gain compared to the non-ideal condition ($K = 0.05$ and $\sigma_e^2 = 0.001$). Also, the effect of HWI and ipCSI was higher with three users compared to the two users. Increasing the number of users reduces the power allocation of the other users which effect the SIC and the signal detection. It recommends that the use of a lower number of users is better to achieve higher performance gain.

In order to examine the impact of HWI and ipCSI, in Fig. 9, we evaluate the impact of the HWI and ipCSI on the considered system in the presence of ipSIC when $SNR = 20$ dB, $l = 3$ and $j = 3$. We observe that both HWI and ipCSI have a negative impact on the system throughput

performance. In Fig. 9 (a), we can easily see that increasing the ipCSI factor decreases system throughput faster, while as can be seen in Fig. 9 (b), an increase in the HWI factor decreases system performance to a lesser extent. Accordingly, system performance is affected by channel estimation error much more than HWI. Also, the HWI and ipCSI weaken the SIC to detect users' signals.

V. CONCLUSION

In this paper, we examine the performance of the OP and system throughput of the uplink SIMO-NOMA system with multiple relays, taking into account practical considerations such as HWI, ipCSI, and ipSIC. By deriving mathematical expressions for the OP and system throughput, we demonstrate that the analytical results match the simulation results. In addition, we discuss the effect of the HWI, ipCSI, and ipSIC on the performance of the uplink SIMO-CNOMA with multiple relays and its crucial role in the system. The findings reveal that irrespective of the number of relays and antennas employed under HWI, ipCSI and ipSIC

conditions, the presence of a high number of users reduces the performance of the system. A lower number of users is better for high-performance gain with fewer errors. The ipCSI has a higher impact on the performance compared to HWI on the considered system. However, the system performance improves as the number of antennas and relays increases. This paper can give valuable insights into the practical implementation of the uplink SIMO-CNOMA system. For future work, it is important to take into account the investigation of multiple input multiple output (MIMO)

technology during both phases in the uplink CNOMA to enhance the system's performance.

APPENDIX A

The OP of the U_j in the first phase is presented in (24). Hence, we can calculate the term $\prod_{m=1}^{Nr} Pr\left(\gamma_{j,I}^{\{m,R_l\}} < \gamma_{th,j}\right)$ of (24) as given in (35), as shown at the bottom of the page. By using the PDF and CDF, we determine (35) as given in (36), as shown at the bottom of the page.

$$
\prod_{m=1}^{Nr} Pr\left(\gamma_{j,I}^{\{m,R_l\}} < \gamma_{th,j}\right)
$$
$$
= \prod_{m=1}^{Nr} Pr\left(\gamma_{j,I}^{\{m,R_l\}} < \gamma_{th,j}\right)
$$
$$
= \prod_{m=1}^{Nr} Pr\left(|\tilde{h}_j^{\{m,R_l\}}|^2 < \frac{\gamma_{th,j}\sum_{j+1}(\alpha_{j+1} + k_{j+1}^{\{m,R_l\}2})P|\tilde{h}_{j+1}^{\{m,R_l\}}|^2 + \gamma_{th,j}\sum_i^{j-1}\varsigma\alpha_i P|\tilde{h}_i^{\{m,R_l\}}|^2 + \gamma_{th,j}\psi_I}{P(\alpha_j - \gamma_{th,j}k_j^{\{m,R_l\}2})}\right). \tag{35}
$$

$$
\prod_{m=1}^{Nr} Pr\left(\gamma_{j,I}^{\{m,R_l\}} < \gamma_{th,j}\right)
$$
$$
= \prod_{m=1}^{Nr}(1 - \exp\left(-\frac{\gamma_{th,j}z_j}{P(\alpha_j - \gamma_{th,j}k_j^{\{m,R_l\}2})\lambda_{h_j^{\{m,R_l\}}}}\right)
$$
$$
\times \int_0^\infty \exp\left(-(\frac{\gamma_{th,j}(\varsigma\alpha_{(j-1)} + k_{j-1}^{\{m,R_l\}2}) P Y_{|\tilde{h}_{(j-1)}^{\{m,R_l\}}|^2}}{P(\alpha_j - \gamma_{th,j}k_j^{\{m,R_l\}2})\lambda_{h_j^{\{m,R_l\}}}})\right) \times \int_0^\infty \exp\left(-(\frac{\gamma_{th,j}(\alpha_{j+1} + k_{j+1}^{\{m,R_l\}2}) P Y_{|\tilde{h}_{j+1}^{\{m,R_l\}}|^2}}{P(\alpha_j - \gamma_{th,j}k_j^{\{m,R_l\}2})\lambda_{h_j^{\{m,R_l\}}}})\right)
$$
$$
\times \frac{\exp\left(\frac{Y_{|\tilde{h}_{j+1}^{\{m,R_l\}}|^2}}{\lambda_{h_{j+1}^{\{m,R_l\}}}}\right)}{\lambda_{h_{j+1}^{\{m,R_l\}}}}dY_{|\tilde{h}_{j+1}^{\{m,R_l\}}|^2} \frac{\exp\left(\frac{Y_{|\tilde{h}_{j-1}^{\{m,R_l\}}|^2}}{\lambda_{h_{j-1}^{\{m,R_l\}}}}\right)}{\lambda_{h_{j-1}^{\{m,R_l\}}}}dY_{|\tilde{h}_{j-1}^{\{m,R_l\}}|^2}
$$
$$
\times \int_0^\infty \exp\left(-(\frac{\gamma_{th,j}(\varsigma\alpha_{j-2} + k_{j-2}^{\{m,R_l\}2}) P Y_{|\tilde{h}_{j-2}^{\{m,R_l\}}|^2}}{P(\alpha_j - \gamma_{th,j}k_j^{\{m,R_l\}2})\lambda_{h_j^{\{m,R_l\}}}})\right) \times \int_0^\infty \exp\left(-(\frac{\gamma_{th,j}(\alpha_{j+2} + k_{j+2}^{\{m,R_l\}2}) P Y_{|\tilde{h}_{j+2}^{\{m,R_l\}}|^2}}{P(\alpha_j - \gamma_{th,j}k_j^{\{m,R_l\}2})\lambda_{h_j^{\{m,R_l\}}}})\right)
$$
$$
\times \frac{\exp\left(\frac{Y_{|\tilde{h}_{j+2}^{\{m,R_l\}}|^2}}{\lambda_{h_{j+2}^{\{m,R_l\}}}}\right)}{\lambda_{h_{j+2}^{\{m,R_l\}}}}dY_{|\tilde{h}_{j+2}^{\{m,R_l\}}|^2} \frac{\exp\left(\frac{Y_{|\tilde{h}_{j-2}^{\{m,R_l\}}|^2}}{\lambda_{h_{j-2}^{\{m,R_l\}}}}\right)}{\lambda_{h_{j-2}^{\{m,R_l\}}}}dY_{|\tilde{h}_{j-2}^{\{m,R_l\}}|^2}
$$
$$
\ldots \times \int_0^\infty \exp\left(-(\frac{\gamma_{th,j}(\varsigma\alpha_{J-1} + k_{J-1}^{\{m,R_l\}2}) P Y_{|\tilde{h}_{J-1}^{\{m,R_l\}}|^2}}{P(\alpha_j - \gamma_{th,j}k_j^{\{m,R_l\}2})\lambda_{h_j^{\{m,R_l\}}}})\right) \times \int_0^\infty \exp\left(-(\frac{\gamma_{th,j}(\alpha_J + k_J^{\{m,R_l\}2}) P Y_{|\tilde{h}_J^{\{m,R_l\}}|^2}}{P(\alpha_j - \gamma_{th,j}k_j^{\{m,R_l\}2})\lambda_{h_j^{\{m,R_l\}}}})\right)
$$
$$
\times \frac{\exp\left(\frac{Y_{|\tilde{h}_J^{\{m,R_l\}}|^2}}{\lambda_{h_J^{\{m,R_l\}}}}\right)}{\lambda_{h_J^{\{m,R_l\}}}}dY_{|\tilde{h}_J^{\{m,R_l\}}|^2} \frac{\exp\left(\frac{Y_{|\tilde{h}_{J-1}^{\{m,R_l\}}|^2}}{\lambda_{h_{J-1}^{\{m,R_l\}}}}\right)}{\lambda_{h_{J-1}^{\{m,R_l\}}}}dY_{|\tilde{h}_{J-1}^{\{m,R_l\}}|^2}. \tag{36}
$$

$$\prod_{m=1}^{Nr} Pr\left(\gamma_{j,I}^{\{m,R_l\}} < \gamma_{th,j}\right) = \prod_{m=1}^{Nr}(1 - \exp\left(-\frac{\gamma_{th,j}z_j}{P(\alpha_j - \gamma_{th,j}k_j^{\{m,R_l\}^2})\lambda_{h_j^{\{m,R_l\}}}}\right)$$

$$\times \frac{P(\alpha_j - \gamma_{th,j}k_j^{\{m,R_l\}^2})\lambda_{h_j^{\{m,R_l\}}}}{P(\alpha_j - \gamma_{th,j}k_j^{\{m,R_l\}^2})\lambda_{h_j^{\{m,R_l\}}} + \gamma_{th,j}(\alpha_{j+1} + k_{j+1}^{\{m,R_l\}^2})P\,\lambda_{h_{j+1}^{\{m,R_l\}}}}$$

$$\times \frac{P(\alpha_j - \gamma_{th,j}k_j^{\{m,R_l\}^2})\lambda_{h_j^{\{m,R_l\}}}}{P(\alpha_j - \gamma_{th,j}k_j^{\{m,R_l\}^2})\lambda_{h_j^{\{m,R_l\}}} + \gamma_{th,j}(\varsigma\alpha_{(j-1)} + k_{j-1}^{\{m,R_l\}^2})P\,\lambda_{h_{j-1}^{\{m,R_l\}}}}$$

$$\times \frac{P(\alpha_j - \gamma_{th,j}k_j^{\{m,R_l\}^2})\lambda_{h_j^{\{m,R_l\}}}}{P(\alpha_j - \gamma_{th,j}k_j^{\{m,R_l\}^2})\lambda_{h_j^{\{m,R_l\}}} + \gamma_{th,j}(\alpha_{j+2} + k_{j+2}^{\{m,R_l\}^2})P\,\lambda_{h_{j+2}^{\{m,R_l\}}}}$$

$$\times \frac{P(\alpha_j - \gamma_{th,j}k_j^{\{m,R_l\}^2})\lambda_{h_j^{\{m,R_l\}}}}{P(\alpha_j - \gamma_{th,j}k_j^{\{m,R_l\}^2})\lambda_{h_j^{\{m,R_l\}}} + \gamma_{th,j}(\varsigma\alpha_{j-2} + k_{j-2}^{\{m,R_l\}^2})P\,\lambda_{h_{j-2}^{\{m,R_l\}}}}$$

$$\vdots$$

$$\times \frac{P(\alpha_j - \gamma_{th,j}k_j^{\{m,R_l\}^2})\lambda_{h_j^{\{m,R_l\}}}}{P(\alpha_j - \gamma_{th,j}k_j^{\{m,R_l\}^2})\lambda_{h_j^{\{m,R_l\}}} + \gamma_{th,j}(\alpha_J + k_J^{\{m,R_l\}^2})P\,\lambda_{h_J^{\{m,R_l\}}}})$$

$$\times \frac{P(\alpha_j - \gamma_{th,j}k_j^{\{m,R_l\}^2})\lambda_{h_j^{\{m,R_l\}}}}{P(\alpha_j - \gamma_{th,j}k_j^{\{m,R_l\}^2})\lambda_{h_j^{\{m,R_l\}}} + \gamma_{th,j}(\varsigma\alpha_{(J-1)} + k_{J-1}^{\{m,R_l\}^2})P\,\lambda_{h_{J-1}^{\{m,R_l\}}}}). \tag{37}$$

The integral of (36) can be calculated as in [38]. Hence, we can obtain (36) as given in (37), as shown at the top of the page. The proof is completed.

REFERENCES

[1] L. Dai, B. Wang, Z. Ding, Z. Wang, S. Chen, and L. Hanzo, "A survey of non-orthogonal multiple access for 5G," *IEEE Commun. Surveys Tuts.*, vol. 20, no. 3, pp. 2294–2323, 3rd Quart., 2018.

[2] W. Shin, M. Vaezi, B. Lee, D. J. Love, J. Lee, and H. V. Poor, "Non-orthogonal multiple access in multi-cell networks: Theory, performance, and practical challenges," *IEEE Commun. Mag.*, vol. 55, no. 10, pp. 176–183, Oct. 2017.

[3] Y. Saito, A. Benjebbour, Y. Kishiyama, and T. Nakamura, "System-level performance evaluation of downlink non-orthogonal multiple access (NOMA)," in *Proc. IEEE Int. Symp. Pers., Indoor Mobile Radio Commun. (PIMRC)*, Sep. 2013, pp. 611–615.

[4] Z. Yang, Z. Ding, P. Fan, and N. Al-Dhahir, "A general power allocation scheme to guarantee quality of service in downlink and uplink NOMA systems," *IEEE Trans. Wireless Commun.*, vol. 15, no. 11, pp. 7244–7257, Nov. 2016.

[5] X. Tian, Q. Li, X. Li, H. Peng, C. Zhang, K. M. Rabie, and R. Kharel, "I/Q imbalance and imperfect SIC on two-way relay NOMA systems," *Electronics*, vol. 9, no. 2, p. 249, Feb. 2020.

[6] A. Agarwal, R. Chaurasiya, S. Rai, and A. K. Jagannatham, "Outage probability analysis for NOMA downlink and uplink communication systems with generalized fading channels," *IEEE Access*, vol. 8, pp. 220461–220481, 2020.

[7] J. Wang, B. Xia, K. Xiao, Y. Gao, and S. Ma, "Outage performance analysis for wireless non-orthogonal multiple access systems," *IEEE Access*, vol. 6, pp. 3611–3618, 2018.

[8] S. A. Tegos, P. D. Diamantoulakis, J. Xia, L. Fan, and G. K. Karagiannidis, "Outage performance of uplink NOMA in land mobile satellite communications," *IEEE Wireless Commun. Lett.*, vol. 9, no. 10, pp. 1710–1714, Oct. 2020.

[9] Y. Gao, B. Xia, Y. Liu, Y. Yao, K. Xiao, and G. Lu, "Analysis of the dynamic ordered decoding for uplink NOMA systems with imperfect CSI," *IEEE Trans. Veh. Technol.*, vol. 67, no. 7, pp. 6647–6651, Jul. 2018.

[10] F. Khennoufa, K. Abdellatif, and F. Kara, "Bit error rate and outage probability analysis for multi-hop decode-and-forward relay-aided NOMA with imperfect SIC and imperfect CSI," *AEU - Int. J. Electron. Commun.*, vol. 147, Apr. 2022, Art. no. 154124.

[11] S. M. Ibraheem, W. Bedawy, W. Saad, and M. Shokair, "Outage performance of NOMA-based DF relay sharing networks over Nakagami-*m* fading channels," in *Proc. 13th Int. Conf. Comput. Eng. Syst. (ICCES)*, Dec. 2018, pp. 512–517.

[12] Z. Ding, M. Peng, and H. V. Poor, "Cooperative non-orthogonal multiple access in 5G systems," *IEEE Commun. Lett.*, vol. 19, no. 8, pp. 1462–1465, Aug. 2015.

[13] Z. Wei, L. Dai, D. W. K. Ng, and J. Yuan, "Performance analysis of a hybrid downlink-uplink cooperative NOMA scheme," in *Proc. IEEE 85th Veh. Technol. Conf. (VTC Spring)*, Jun. 2017, pp. 1–7.

[14] V. Singh, V. Bankey, and P. K. Upadhyay, "Underlay cognitive hybrid satellite-terrestrial networks with cooperative-NOMA," in *Proc. IEEE Wireless Commun. Netw. Conf. (WCNC)*, May 2020, pp. 1–6.

[15] Z. Ding, H. Dai, and H. V. Poor, "Relay selection for cooperative NOMA," *IEEE Wireless Commun. Lett.*, vol. 5, no. 4, pp. 416–419, Aug. 2016.

[16] Z. Yang, Z. Ding, Y. Wu, and P. Fan, "Novel relay selection strategies for cooperative NOMA," *IEEE Trans. Veh. Technol.*, vol. 66, no. 11, pp. 10114–10123, Nov. 2017.

[17] H. Lei, Z. Yang, K.-H. Park, I. S. Ansari, Y. Guo, G. Pan, and M.-S. Alouini, "Secrecy outage analysis for cooperative NOMA systems with relay selection schemes," *IEEE Trans. Commun.*, vol. 67, no. 9, pp. 6282–6298, Sep. 2019.

[18] J. Men and J. Ge, "Non-orthogonal multiple access for multiple-antenna relaying networks," *IEEE Commun. Lett.*, vol. 19, no. 10, pp. 1686–1689, Oct. 2015.

[19] T. N. Do, D. B. D. Costa, T. Q. Duong, and B. An, "Improving the performance of cell-edge users in MISO-NOMA systems using TAS and SWIPT-based cooperative transmissions," *IEEE Trans. Green Commun. Netw.*, vol. 2, no. 1, pp. 49–62, Mar. 2018.

[20] H. Semira and F. Kara, "Error performance of uplink SIMO-NOMA with joint maximum-likelihood and adaptive M-PSK," in *Proc. IEEE Int. Black Sea Conf. Commun. Netw. (BlackSeaCom)*, May 2021, pp. 1–6.

[21] T. Schenk, *RF Imperfections in High-Rate Wireless Systems: Impact and Digital Compensation*. Dordrecht, The Netherlands: Springer, 2008.

[22] S. Beddiaf, A. Khelil, F. Khennoufa, and K. Rabie, "On the impact of IQI on cooperative NOMA with direct links in the presence of imperfect CSI," *Phys. Commun.*, vol. 56, Feb. 2023, Art. no. 101952.

[23] X. Li, M. Zhao, M. Liu, L. Li, Z. Ding, and A. Nallanathan, "Secrecy analysis of ambient backscatter NOMA systems under I/Q imbalance," *IEEE Trans. Veh. Technol.*, vol. 69, no. 10, pp. 12286–12290, Oct. 2020.

[24] F. Ding, H. Wang, S. Zhang, and M. Dai, "Impact of residual hardware impairments on non-orthogonal multiple access based amplify-and-forward relaying networks," *IEEE Access*, vol. 6, pp. 15117–15131, 2018.

[25] X. Li, J. Li, J. Jin, and L. Li, "Performance analysis of relaying systems over Nakagami-*m* fading with transceiver hardware impairments," *J. Xidian Univ.*, vol. 25, no. 3, pp. 135–140, Oct. 2017.

[26] S. Beddiaf, A. Khelil, F. Khennoufa, F. Kara, H. Kaya, X. Li, K. Rabie, and H. Yanikomeroglu, "A unified performance analysis of cooperative NOMA with practical constraints: Hardware impairment, imperfect SIC and CSI," *IEEE Access*, vol. 10, pp. 132931–132948, 2022.

[27] K. Guo, C. Dong, and K. An, "NOMA-based cognitive satellite terrestrial relay network: Secrecy performance under channel estimation errors and hardware impairments," *IEEE Internet Things J.*, vol. 9, no. 18, pp. 17334–17347, Sep. 2022.

[28] Y. Akhmetkaziyev, G. Nauryzbayev, S. Arzykulov, A. M. Eltawil, K. M. Rabie, and X. Li, "Performance of NOMA-enabled cognitive satellite-terrestrial networks with non-ideal system limitations," *IEEE Access*, vol. 9, pp. 35932–35946, 2021.

[29] X. Li, Y. Zheng, M. D. Alshehri, L. Hai, V. Balasubramanian, M. Zeng, and G. Nie, "Cognitive AmBC-NOMA IoV-MTS networks with IQI: Reliability and security analysis," *IEEE Trans. Intell. Transp. Syst.*, pp. 1–12, 2021.

[30] D. Cui, G. Huang, Y. Zheng, H. Guo, J. Li, and X. Li, "Performance analysis of ABCom NOMA systems for 6G with generalized hardware impairments," *Phys. Commun.*, vol. 54, Oct. 2022, Art. no. 101851.

[31] F. Khennoufa, A. Khelil, S. Beddiaf, F. Kara, K. Rabie, H. Kaya, A. Emir, S. Ikki, and H. Yanikomeroglu, "Wireless powered cooperative communication network for dual-hop uplink NOMA with IQI and SIC imperfections," *IEEE Access*, vol. 11, pp. 76506–76523, 2023.

[32] D. Zou, D. Deng, Y. Rao, X. Li, and K. Yu, "Relay selection for cooperative NOMA system over correlated fading channel," *Phys. Commun.*, vol. 35, Aug. 2019, Art. no. 100702.

[33] A. Afana, N. Abu-Ali, and S. Ikki, "On the joint impact of hardware and channel imperfections on cognitive spatial modulation MIMO systems: Cramer–Rao bound approach," *IEEE Syst. J.*, vol. 13, no. 2, pp. 1250–1261, Jun. 2019.

[34] M. Shen, Z. Huang, X. Lei, and L. Fan, "BER analysis of NOMA with max-min relay selection," *China Commun.*, vol. 18, no. 7, pp. 172–182, Jul. 2021.

[35] G. Nauryzbayev, S. Arzykulov, T. A. Tsiftsis, and M. Abdallah, "Performance of cooperative underlay CR-NOMA networks over Nakagami-*m* channels," in *Proc. IEEE Int. Conf. Commun. Workshops (ICC Workshops)*, May 2018, pp. 1–6.

[36] H. Yahya, E. Alsusa, and A. Al-Dweik, "Exact BER analysis of NOMA with arbitrary number of users and modulation orders," *IEEE Trans. Commun.*, vol. 69, no. 9, pp. 6330–6344, Sep. 2021.

[37] K. Ferdi and K. Hakan, "A true power allocation constraint for non-orthogonal multiple access with M-QAM signalling," in *Proc. IEEE Microw. Theory Techn. Wireless Commun.*, vol. 1, Oct. 2020, pp. 7–12.

[38] X. Xie, J. Liu, J. Huang, and S. Zhao, "Ergodic capacity and outage performance analysis of uplink full-duplex cooperative NOMA system," *IEEE Access*, vol. 8, pp. 164786–164794, 2020.
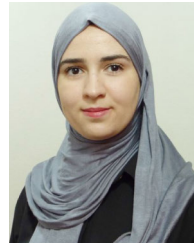
SAFIA BEDDIAF received the B.S. and master's degrees in telecommunication engineering from the University of 8 mai 1945, Guelma, Algeria, in 2014 and 2019, respectively. She is currently pursuing the Ph.D. degree with Echahid Hamma Lakhdar University, El Oued, Algeria. Her research interests include wireless communications networks, non-orthogonal multiple access (NOMA), hardware impairment, IQ imbalance, cooperative communication, and RIS.

ABDELLATIF KHELIL received the B.S. and M.S. degrees in communication engineering from the University of Setif, Algeria, in 2005 and 2009, respectively, and the Ph.D. degree in the field of communication engineering from the University of Setif with the collaboration of UQO University, Canada. He has been with the Electrical Engineering Department, El-Oued University, Algeria, since 2011, where he is currently an Associate Professor in communication engineering. He has numerous publications in peer-reviewed journals and conferences. He is serving as a Reviewer in a number of international journals, including IEEE ACCESS, IEEE WIRELESS COMMUNICATION LETTERS, *Physical Communications*, *International Journal of Electronics*, *International Journal of Communication Systems*, and *Transactions on Emerging Telecommunications Technologies*. His research interests include wireless communications, cellular communications (5G, B5G and 6G), MIMO systems, mm-waves propagation, THz communications, new waveforms, NOMA, and RIS.

FAICAL KHENNOUFA received the B.S. and master's degrees in telecommunication engineering from the University of Djillali Liabes, Sidi Bel Abbas, Algeria, in 2012 and 2017, respectively. He is currently pursuing the Ph.D. degree with Echahid Hamma Lakhdar University, El Oued, Algeria. His research interests include wireless communications networks, non-orthogonal multiple access (NOMA), cooperative communication, IQ imbalance, RF impairments, spatial modulation (SM), energy harvesting, RIS, and TNT networks.

FERDI KARA (Senior Member, IEEE) received the B.Sc. degree (Hons.) in electronics and communication engineering from Suleyman Demirel University, Isparta, Turkey, in 2011, and the M.Sc. and Ph.D. degrees in electrical and electronics engineering from Zonguldak Bülent Ecevit University (ZBEU), Zonguldak, Turkey, in 2015 and 2019, respectively. Since 2011, he has been working with the Wireless Communication Technologies Research Laboratory. He is currently an Assistant Professor with the Department of Computer Engineering, ZBEU. He was a Senior Research Associate with the Department of Systems and Computer Engineering, Carleton University, Ottawa, ON, Canada between 2021 to 2023. His research interests include wireless communications specified with NOMA, MIMO/RIS/LIS systems, cooperative communication, index modulations, energy harvesting, faster than Nyquist signaling, aerial networks, and machine learning algorithms in communications.

Dr. Kara's Ph.D. thesis is awarded the Best Ph.D. Thesis by IEEE Türkiye Section, in 2021, and Turkish Academy of Science (TüBA), in 2022. He has been listed among World's Top %2 Scientist List by Stanford University and Elsevier, in 2021. He has been awarded the 2020 Premium Award for Best Paper in IET Communications and the Best Early Researcher Paper Award in IEEE Blakcseacom2021. He received the Best Editor Certificate by IEEE Communications Letters in 2022. He also received an Exemplary Reviewer Certificate from IEEE Transactions on Communications in 2022, and from IEEE Communications Letters from 2019 to 2022 in a row of four years. He regularly serves as a Technical Program Committee Member in flagship IEEE conferences (e.g., ICC, Globecom, VTC, and WCNC). He is also an Editor of IEEE Communications Letters, an Associate Editor of EURASIP *Journal of Wireless Communications and Networking*, and an Area Editor of *Physical Communication* (Elsevier).

KHALED RABIE (Senior Member, IEEE) received the M.Sc. and Ph.D. degrees in electrical and electronic engineering from The University of Manchester, in 2011 and 2015, respectively. He is currently a Reader with the Department of Engineering, Manchester Metropolitan University (MMU), U.K. He has worked as a part of several largescale industrial projects and he has published more than 200 journals and conference papers (mostly IEEE). His current research interests include designing and developing next-generation wireless communication systems. He serves regularly on the Technical Program Committee (TPC) for several major IEEE conferences, such as GLOBECOM, ICC, and VTC. He has received many awards over the past few years in recognition of his research contributions, including the Best Paper Awards at the 2021 IEEE CITS and the 2015 IEEE ISPLC, and the IEEE Access Editor of the Month Award, in August 2019. He is serving as an Editor for IEEE COMMUNICATIONS LETTERS, an Editor for *IEEE Internet of Things Magazine*, an Associate Editor for IEEE Access, and an Executive Editor for the *Transactions on Emerging Telecommunications Technologies* (Wiley). He has guest-edited many special issues in journals, including *IEEE Wireless Communications Magazine*, in 2021, *Electronics*, in 2021, *Sensors*, in 2020, and IEEE Access, in 2019. He is also a fellow of the U.K. Higher Education Academy (FHEA).

XINGWANG LI (Senior Member, IEEE) received the M.Sc. degree from the University of Electronic Science and Technology of China, in 2010, and the Ph.D. degree from the Beijing University of Posts and Telecommunications, in 2015. From 2010 to 2012, he was with Comba Telecom Ltd., Guangzhou China, as an Engineer. He spent one year, from 2017 to 2018, as a Visiting Scholar with Queen's University Belfast, Belfast, U.K. He is currently an Associate Professor with the School of Physics and Electronic Information Engineering, Henan Polytechnic University, Jiaozuo, China. He was a Visiting Scholar with the State Key Laboratory of Networking and Switching Technology, Beijing University of Posts and Telecommunications, from 2016 to 2018. His research interests include MIMO communication, cooperative communication, hardware constrained communication, non-orthogonal multiple access, physical layer security, unmanned aerial vehicles, and the Internet of Things. He has served as many TPC members, such as the IEEE GLOBECOM, IEEE WCNC, IEEE VTC, and IEEE ICCC. He has also served as the Co-Chair for the IEEE/IET CSNDSP 2020 of the Green Communications and Networks Track. He also serves as an Editor on the Editorial Board for IEEE Access, *Computer Communications*, *Physical Communication*, *KSII Transactions on Internet and Information Systems*, and *IET Quantum Communication*. He is also the Lead Guest Editor for the Special Issue on UAV-Enabled B5G/6G Networks: Emerging Trends and Challenges of *Physical Communication*, Special Issue on Recent Advances in Physical Layer Technologies for the 5G-Enabled Internet of Things of *Wireless Communications and Mobile Computing*, and Special Issue on Recent Advances in Multiple Access for 5G-Enabled IoT of *Security and Communication Networks*.

HAKAN KAYA received the B.Sc., M.Sc., and Ph.D. degrees in electrical and electronics engineering from Zonguldak Karaelmas University, Turkey, in 2007, 2010, and 2015, respectively. Since 2015, he has been with Zonguldak Bülent Ecevit University as an Assistant Professor and the Head of the Wireless Communication Technologies Research Laboratory (WCTLab). His research interests include cooperative communication, NOMA, turbo coding, and machine learning.
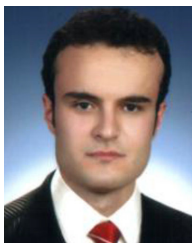
AHMET EMIR received the B.Sc. degree in electronics and communications engineering from Kocaeli University, Turkey, in 2007, and the M.Sc. and Ph.D. degrees in electrical and electronics engineering from Zonguldak Bülent Ecevit University, Turkey, in 2014 and 2021, respectively. Since 2012, he has been with the Distance Education Research and Application Center (DERAC), Zonguldak Bülent Ecevit University, as a Lecturer. His research interests include NOMA and machine learning in physical layer.

HALIM YANIKOMEROGLU (Fellow, IEEE) is currently a Chancellor's Professor with the Department of Systems and Computer Engineering, Carleton University, Canada. His research interests include wireless communications and networks. His research group has made substantial contributions to 4G/5G wireless technologies. His group's current focus is the wireless infrastructure for the 6G and B6G era with terrestrial, aerial (HAPS and UAV), and satellite network elements.

His extensive collaboration with industry resulted in 39 granted patents. He is a fellow of the Engineering Institute of Canada (EIC) and Canadian Academy of Engineering (CAE). He is an IEEE Distinguished Speaker for ComSoc and VTS. He has given over 150 keynotes, tutorials, and invited seminars in the last ten years. He is serving as the Steering Committee Chair of IEEE Wireless Communications and Networking Conference (WCNC). He is also a member of the IEEE ComSoc Conference Council and IEEE PIMRC Steering Committee. He has served as the general chair and the technical program chair of several IEEE conferences. He has also served in the editorial boards of various IEEE periodicals. He received several awards for his research, teaching, and service, including the IEEE ComSoc Fred W. Ellersick Prize, in 2021, the IEEE VTS Stuart Meyer Memorial Award, in 2020, and the IEEE ComSoc Wireless Communications TC Recognition Award, in 2018. He received best paper awards at IEEE ICC 2021 and IEEE WISEE 2021.

• • •